Int. J. Electrochem. Sci., 13 **(2018)** 8953 – 8959, doi: 10.20964/2018.09.37

International Journal of
ELECTROCHEMICAL
SCIENCE
www.electrochemsci.org

Short Communication

Performance of Mg-air Battery Based on AZ31 Mg Alloy Sheets with Different Grain Sizes

Yanchun Zhao [1], *Guangsheng Huang* [2,3,*], *Cheng Zhang* [2],
Cheng Peng [1] *and Fusheng Pan* [2,3]

[1] Chongqing Key Laboratory of Extraordinary Bond Engineering and Advanced Materials Technology, Yangtze Normal University, Chongqing 408100, China
[2] State Key Laboratory of Mechanical Transmission, Chongqing University, Chongqing 400044, China
[3] National Engineering Research Center for Magnesium Alloys，Chongqing University, Chongqing 400044, China
[*]E-mail: gshuang@cqu.edu.cn

Received: 24 April 2018 / *Accepted:* 7 June 2018 / *Published:* 5 August 2018

Mg-air batteries have attracted great attention recently because of their high energy density and lack of pollution. This paper studied the effect of grain sizes on the performance of Mg-air batteries. AZ31 Mg alloy sheets with different grain sizes were obtained through cold-rolling and annealing. The potentiodynamic polarization curves revealed that AZ31 Mg alloy sheets with fine grain sizes have higher electrochemical activity and better corrosion resistance compared to AZ31 Mg alloy sheets with coarse grain sizes. Mg-air batteries based on processed AZ31 alloy sheets were prepared, and the battery performances were investigated by a constant-current discharging test. The results show that the Mg-air battery based on a fine-grain anode exhibited a preferable discharge performance, including a higher discharge voltage and a higher anodic efficiency that those of the battery is a coarse-grain anode.

Keywords: Mg alloys, Grain size, Electrochemical property, Mg-air battery, Anodic efficiency, Discharge voltage

1. INTRODUCTION

Metal-air batteries have drawn much attention for their high theoretical energy and lack of pollution [1-3]. The negative standard electrode potential, high Faradic capacity and low density of magnesium make it attractive as a potential anode material in metal-air batteries. However, large-scale commercial applications of Mg-air batteries have been significantly limited because of the high corrosion rate and polarization of the Mg anodes in NaCl electrolytes.

Tremendous efforts, concentrating mainly on alloying treatment [4-8] and electrolyte modification [2, 9-11], have been devoted to solving the current limitations. The microstructures is known to have a significant effect on the mechanical properties and electrochemical performance of magnesium alloys and can be regulated in various ways [12-15]. Therefore, improving the microstructure of Mg anodes may be a good way to improve the discharge performance of Mg-air batteries. In previous studies, we found the Mg-air batteries with an appropriate concentration of twins have a high average discharge voltage and a short voltage lag time [16]. Grain size has a great impact on the corrosion behaviour and electrochemical activity of Mg alloys [13, 17]. That is, the grain size may have a strong influence on the performance of Mg-air batteries because of their effects on the corrosion behaviour and polarization of the Mg anodes. However, relatively few studies have been conducted on this subject.

Thus, the purpose of this study is to investigate the effect of grain size on the performance of Mg-air batteries. AZ31 Mg alloys with different grain sizes were prepared. Mg-air batteries using these alloys as anodes were fabricated, and battery performance was evaluated.

2. EXPERIENTIAL

Mg-alloy sheets with a chemical composition (in wt%) of 2.72 Al, 0.92 Zn, 0.35 Mn, 0.13 Si and Mg balance were used as the anode materials. The as-received sheets were cold-rolled along the rolling direction with a rolling reduction of 5%. Then, the cold-rolled samples were placed in a furnace and annealed at 350℃ and 450℃ for 2 hours. The samples after the heat treatment were named RA 350 or RA 450, respectively. The optical microstructures of the samples were examined through an optical microscopy. The samples were ground with 1200-grit SIC paper before the polarization and discharge tests. A 3.5 wt% NaCl solution was used as the electrolyte solution. The experiments were performed at 25±2℃.

A three-electrode electrochemical cell was used for the electrochemical measurements. The Mg electrode was used as the working electrode, a platinum electrode was used as the counter electrode, and a saturated calomel electrode was used as the reference electrode. Before the electrochemical measurements, the samples were immersed in an NaCl solution for approximately 30 minutes to guarantee the stability of the solution system. Potentiodynamic polarization curves were measured at a scan rate of 0.5 mV s^{-1}, and the electrochemical impedance spectroscopy (EIS) curves were measured at open circuit potential with a 5 mV sine wave perturbation. The measuring frequency range was 100 kHz-0.1 Hz. ZView software was used to fit the results of the EIS curves.

Mg-air batteries consisting of an anode (AZ31 Mg alloy with different grain sizes), cathode (air electrode with a MnO_2 catalyst) and electrolyte (3.5 wt% NaCl solution) were prepared. Constant-current discharging tests were performed using a battery testing system (BTS-MPTS, China) at a discharge current density of 10 mA cm^{-2}. The anodic efficiencies of the Mg-air batteries were calculated from the weight of the consumed Mg anodes. The anodic efficiencies were calculated using Eq. (1) [18]:

$$\text{Anodic efficiency } (\%) = \frac{i \times A \times t \times M_a}{2F \times W_c} \times 100\% \quad (1)$$

In the above formula, i, t, F, A, M_a and W_c represent the current density (A cm^{-2}), the total discharge time (h), Faraday's constant (96,485 C mol^{-1}), the surface area (cm^2), the atomic mass (g mol^{-1}) of the specimens, and the weight of the consumed Mg, respectively.

3. RESULTS AND DISCUSSION

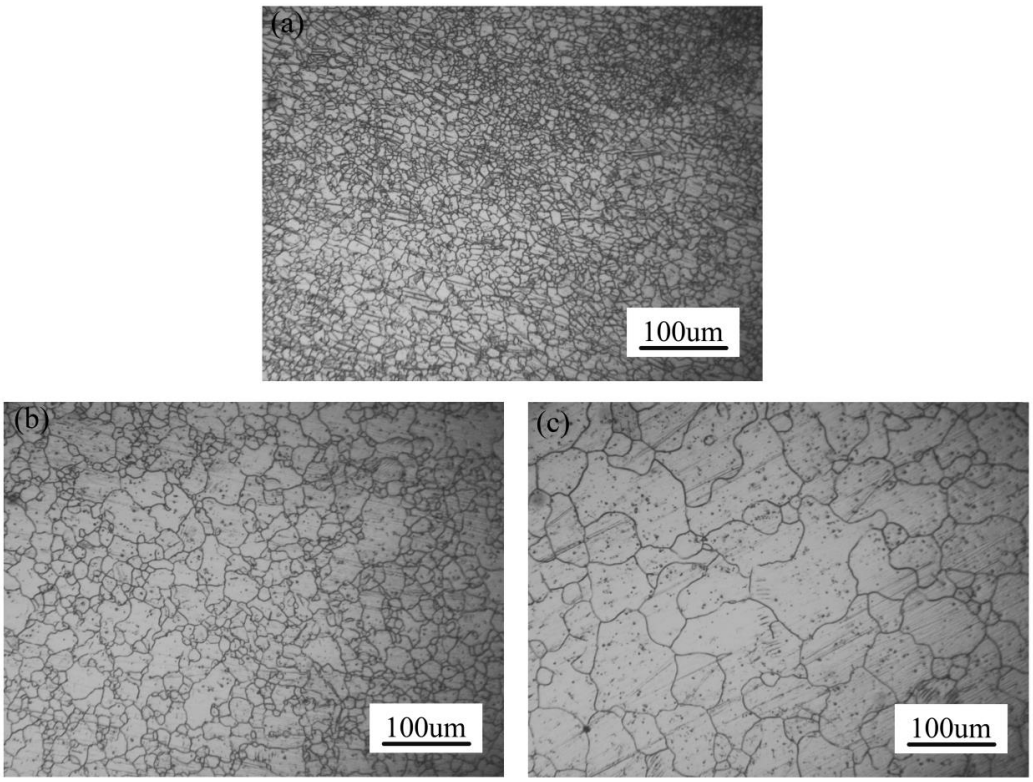

Figure 1. Optical microscopic images of the (a) as-received, (b) RA 350 and (c) RA 450 Mg alloys.

Fig. 1 shows the optical microscopy images of the samples. The average grain sizes of the as-received, RA 350 and RA 450 Mg alloys are 7.5 μm, 20.3 μm and 61.4 μm, respectively. Clearly, the cold-rolling and annealing process led to grain growth in the samples. Fig. 2 shows the potentiodynamic polarization curves of the samples in a 3.5 wt% NaCl solution. The corrosion potentials are -1.50 V, -1.48 V and -1.43 V for the as-received, RA 350 and RA 450 Mg alloys, respectively, indicating that the electrochemical activity of the AZ31 alloy increases with decreasing grain size because grain its boundaries are more active than the grain boundaries in the bulk [16], and a Mg anode with a fine grain size has more grain boundaries than its coarse-grain counterpart.

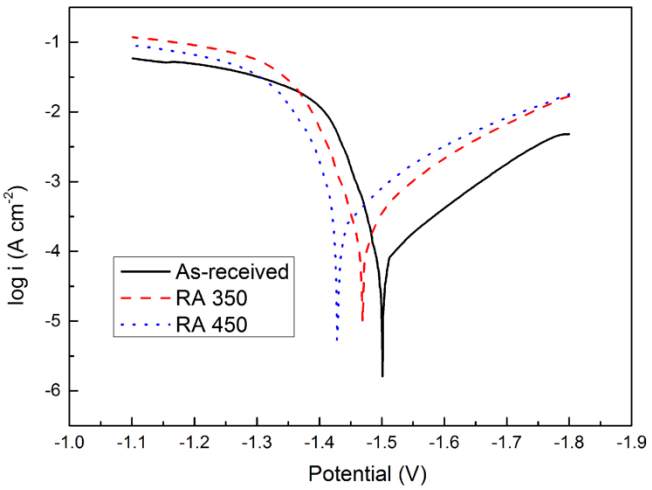

Figure 2. Potentiodynamic polarization curves of the samples in a 3.5 wt% NaCl solution.

The corrosion current densities of the Mg alloys are ordered as follows: as-received < RA 350 < RA 450, which indicates that the corrosion rate of the AZ31 alloy increases with grain size. The grain boundary acts as a physical corrosion barrier in the corrosion process, and thus, the rate of corrosion in the fine-grain microstructure slows compared to the rate of corrosion in the coarse-grain microstructure [13, 16]. Therefore, the alloy with a fine grain size has better corrosion resistance that an alloy with a coarse grain size.

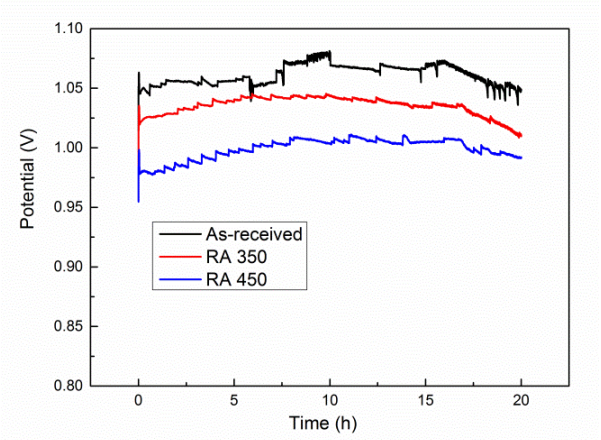

Figure 3. Discharge curves of the Mg-air batteries at a current density of 10 mA cm^{-2}.

Fig. 3 shows the discharge curves of the batteries with different anodes at a current density of 10 mA cm^{-2}. The corresponding discharge performance parameters are shown in Table 1.

Table 1. Discharge performance parameters of the three kinds of Mg-air batteries.

Anodes	Average discharge voltage (V)	Anodic efficiency (%)
As-received	1.06	64.2
RA 350	1.03	56.5
RA 450	0.95	47.6

The average discharge voltages of the Mg anodes are ordered as follows: as-received > RA 350 > RA 450. With decreasing grain size, the average discharge voltages of the Mg-air batteries with the as-received, RA 350 and RA 450 anodes are 1.06 V, 1.03 V and 0.99 V, respectively. The anodic efficiencies of the Mg-air batteries with the as-received, RA 350 and RA 450 anodes are 64.2%, 56.5% and 47.6%, respectively. Overall, the fine-grain Mg anode showed better performance than the coarse-grain Mg anode, which agrees well with the potentiodynamic results.

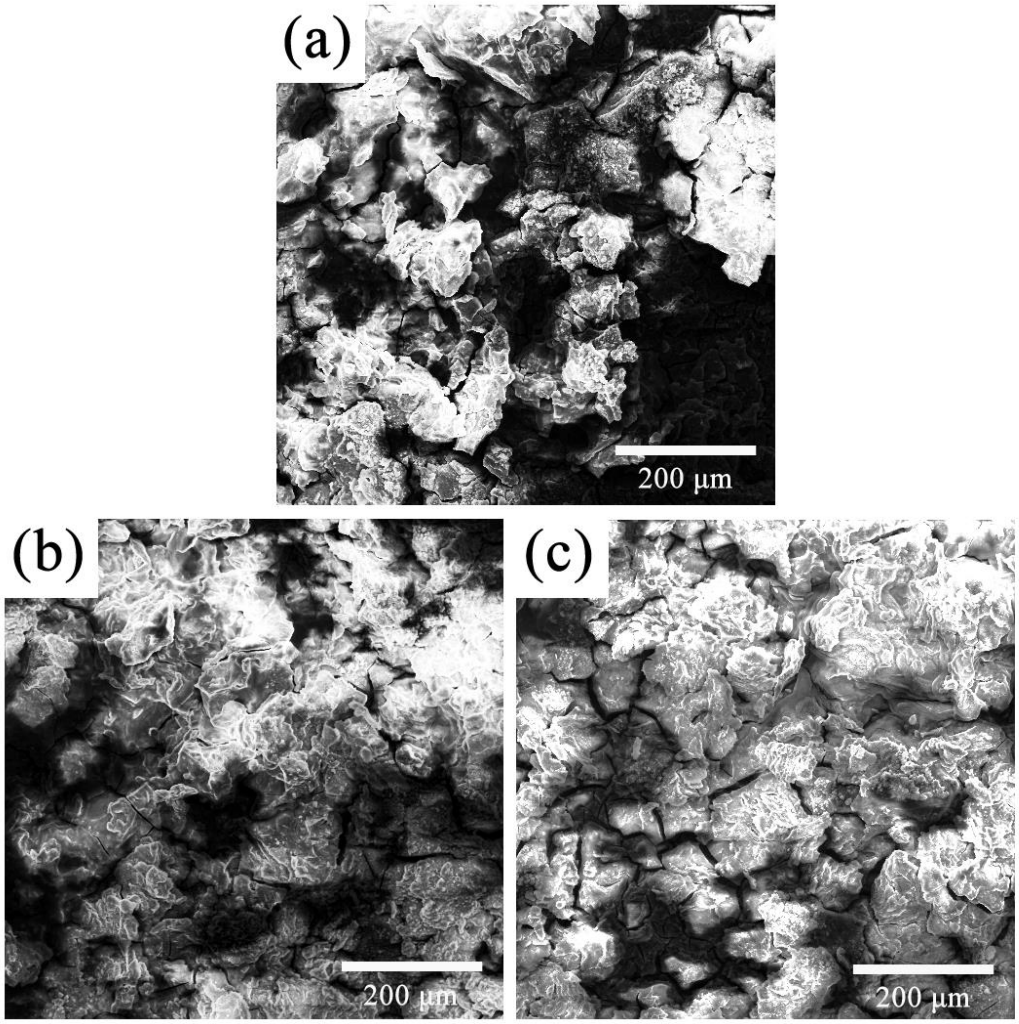

Figure 4. The surface morphologies of (a) as-received, (b) RA 350 and (c) RA 450 anodes after discharging.

Fig. 4. shows the surface morphologies of the three anodes after discharging for 20 hours. The three anodes are all fully covered by the discharge products after the long discharge process. The discharge product film restrains the discharge reaction and reduces the battery performance. However, the grain boundaries with high electrochemical activity may accelerate the fall-off of the discharge products. The Mg anodes with finer grains show discharge product films with many deep grooves. The deep grooves allow the electrolyte to readily penetrate through, which helps improve the battery performance.

Fig. 5(a) shows the EIS curves of the Mg anodes after the discharge tests. The curves consist of two loops. A high-frequency capacitive loop may result from the charge transfer reaction in the electric double layer between the metal surface and the electrolyte solution. The medium frequency capacitive loop is related to ion diffusion [19]. The equivalent circuit of the EIS curves is shown in Fig. 5(b).

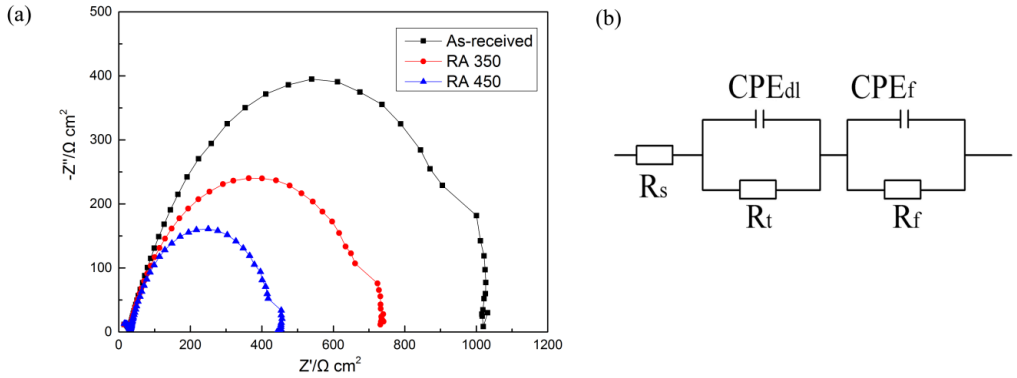

Figure 5. (a) Impedance spectra curves of the Mg anodes after discharging, and (b) the equivalent circuit of the EIS plots.

Due to non-homogeneity in the system, a constant phase element (CPE) is used to replace the capacitance (C). In Fig. 5(b), R_s represents the solution resistance, CPE_{dl} represents the electric double-layer capacity, R_t represents the charge transfer resistance, R_f represents the film resistance and CPE_f represents the film capacity.

Table 2. The EIS fitting results.

Samples	R_s (Ω cm^2)	CPE_{dl}-T (uF cm^{-2})	CPE_{dl}-P (n_{dl})	R_t (Ω cm^2)	CPE_f (uF cm^{-2})	CPE_f-P (n_f)	R_f (Ω cm^2)
As-received	3.57	68.72	0.79	1049	0.44	0.84	29.7
RA 350	3.32	62.31	0.80	714.5	0.21	0.92	26.11
RA 450	2.78	76.61	0.82	423.6	0.26	0.88	31.77

The EIS fitting results are listed in Table 2. Normally, a higher R_t reflects lower corrosion [20]. The R_t value decreases in the following order: as-received > RA 350 > RA 450. The better corrosion resistance of the fine-grain Mg anode leads to higher anodic efficiency.

4. CONCLUSION

The performance of Mg-air batteries based on AZ31 Mg alloys with different grain sizes was investigated in this study. The electrochemical activity of the AZ31 alloy increased with decreasing grain size. The corrosion rate of the AZ31 alloy increased with grain size. A Mg-air battery based on a fine-grain exhibited a high discharge voltage and high anodic efficiency. After the discharge test, the

fine-grain anode showed a high charge transfer resistance, which was closely related to its high anodic efficiency. Therefore, the Mg alloy with a fine grain size was more suitable as an anode material in Mg-air batteries.

ACKNOWLEDGMENTS
This work is supported by the key project of the National Natural Science Foundation of China (No. 51531002) and Fundamental Research Funds for the Central Universities (CDJZR14130009).

References

1. X. Li, H. Lu, S. Yuan, J. Bai, J. Wang, Y. Cao, Q. Hong, *J. Electrochem. Soc*., 164 (2017) A3131.
2. Y. Yan, D. Gunzelmann, C. Pozo-Gonzalo, A.F. Hollenkamp, P.C. Howlett, D.R. Macfarlane, M. Forsyth, *Electrochim. Acta*, 235 (2017) 270.
3. C.S. Li, Y. Sun, F. Gebert, S.L. Chou, *Adv. Energy. Mater*., 7 (2017) 1700869.
4. N. Wang, R. Wang, W. Xiong, J. Zhang, Y. Feng, *J. Mater. Chem*. A, 4 (2016) 8658.
5. S. Yuan, H. Lu, Z. Sun, L. Fan, X. Zhu, W. Zhang, *J. Electrochem. Soc.,* 163 (2016) A1181.
6. N. Wang, R. Wang, Y. Feng, W. Xiong, J. Zhang, M. Deng, *Corros. Sci*., 112 (2016) 13.
7. H.K. Sang, J.H. Park, H.S. Kim, J.J. Kim, O.D. Kwon, Springer International Publishing, 2017 pp413-419.
8. H. Xiong, K. Yu, X. Yin, Y. Dai, Y. Yan, H. Zhu, *J. Alloy. Compd*., 708 (2016) 652.
9. M.M. Dinesh, K. Saminathan, M. Selvam, S. Srither, V. Rajendran, K.V. Kaler, *J. Power Sources*, 276 (2015) 32.
10. F.W. Richey, B.D. Mccloskey, A.C. Luntz, *J. Electrochem. Soc*., 163 (2016) A958.
11. M.A. Deyab, *J. Power Sources*, 325 (2016) 98.
12. R. Ambat, N.N. Aung, W. Zhou, *Corros. Sci.*, 42 (2000) 1433.
13. G.-L. Song, Z. Xu, *Corros. Sci*., 54 (2012) 97.
14. H. Zhang, Y. Liu, J. Fan, H.J. Roven, W. Cheng, B. Xu, H. Dong, *J. Alloy. Compd*., 615 (2014) 687.
15. H. Zhang, Y. Yan, J. Fan, W. Cheng, H.J. Roven, B. Xu, H. Dong, *Mat. Sci. Eng*. A, 618 (2014) 540.
16. G Huang, Y Zhao, Y Wang, H Zhang, F Pan, Mater. Lett., 113 (2013) 46.
17. A. Atrens, G.L. Song, F. Cao, Z. Shi, P.K. Bowen, *J. Magn. Alloy*., 1 (2013) 177.
18. D. Cao, X. Cao, G. Wang, L. Wu, Z. Li, *J. Solid. State. Electr.*, 14 (2010) 851.
19. Y. Ma, N. Li, D. Li, M. Zhang, X. Huang, *J. Power Sources*, 196 (2011) 2346.
20. J. Ma, J. Wen, J. Gao, Q. Li, *J. Power Sources*, 253 (2014) 419.